



Disposable Prussian blue-anchored electrochemical sensor for enzymatic and non-enzymatic multi-analyte detection

Rodrigo Vieira Blasques^{a,b}, Jéssica S. Stefano^a, Jéssica R. Camargo^{a,b}, Luiz R. Guterres e Silva^{a,b}, Laís Canniatti Brazaca^c, Bruno Campos Janegitz^{a,*}

^a Laboratory of Sensors, Nanomedicine and Nanostructured Materials, Federal University of São Carlos, Araras 13600-970, Brazil

^b Department of Physics, Chemistry, and Mathematics, Federal University of São Carlos, Sorocaba, São Paulo 18052-780, Brazil

^c Department of Chemistry and Chemical Biology, Harvard University, Cambridge, MA 02138, United States

ARTICLE INFO

Keywords:

Screen printed electrode
Lab-made conductive ink
Point-of-care
Prussian blue modified electrode
Glucose biosensing

ABSTRACT

The interest in sustainable and low-cost materials for the production of new sensing platforms has been increasing over the time. The possibility of obtaining reliable sensors, on a large scale, easy-to-produce, and cost-effective allows for the development of analytical devices with adequate characteristics for point-of-care analysis. In this context, we present the development of a new low-cost and easy-to-produce disposable electrochemical device composed of a conductive ink modified with Prussian blue for the detection of uric acid, hydrogen peroxide, and glucose. The electrode surface was characterized by scanning electron microscopy coupled with energy dispersive spectroscopy, Fourier-transform infrared spectroscopy, and cyclic voltammetric techniques. Also, the proposed sensors and biosensors were applied for the electrochemical determination of uric acid, hydrogen peroxide, and glucose. The device achieved a linear response ranging from 5.0 to 150.0 $\mu\text{mol L}^{-1}$ for uric acid, with a limit of detection of 0.70 $\mu\text{mol L}^{-1}$ using differential pulse voltammetry. The detection of hydrogen peroxide and glucose was performed using amperometry at a working potential of -0.3 V , which. Hydrogen peroxide sensing presented a linear range varying from 100.0 to 800.0 $\mu\text{mol L}^{-1}$, with a LOD of 31.6 $\mu\text{mol L}^{-1}$. A glucose biosensor was developed after modification of the electrode with a film composed of chitosan, glutaraldehyde, and glucose oxidase, which presented a linear range varying from 50.0 to 500.0 $\mu\text{mol L}^{-1}$, with a LOD of 9.20 $\mu\text{mol L}^{-1}$. Also, the construction of a 3D printed wearable wristband was proposed facing uric acid determination, to show the versatility of the sensor.

1. Introduction

The widespread of low-cost disposable electrochemical platforms became of great interest for clinical analysis. The simplicity, fast response, and possibility of miniaturization provided by these platforms are very attractive characteristics for analytical systems and meet the requirements for the obtention of point-of-care devices (POCDs). The use of POCDs allows the decentralized clinical monitoring of molecules of great interest in clinical analysis, which can decrease the healthcare cost and provide an improvement in the health quality of the patients [1]. In this context, the development and the construction of electrochemical sensors with low-cost conductive inks are presented as an interesting option for the obtention of electrochemical sensors. They are simple, and easy to construct, which are attractive, especially when compared to conventional metallic and carbon-based electrodes, or even

to commercial screen-printed carbon electrodes (SPCEs) [2,3].

The use of conductive inks has been widely explored in the literature for the obtention of new portable, flexible and disposable wearable sensors [4,5]. Recently, the use of diverse compounds has been explored for the obtention of inks, attributing simplicity and low cost [6–8]. In this aspect, nail polish (NP) has been presented as an innovative way to manufacture conductive inks used for the preparation of electrochemical sensors. In addition to the easy obtention and handling, this material presents a low cost and nontoxic composition, containing only polymers, organic solvents, nitrocellulose, and plasticizers [9].

Furthermore, the use of electrochemical sensors based on conductive inks allows versatility to the obtained devices, depending on the substrate employed. It is possible to attribute flexibility to the sensor, by the use of flexible substrates such as polyethylene terephthalate (PET) and silicon rubber [10], stiffness, by the use of glass substrates [11], or even

* Corresponding author.

E-mail address: brunocj@ufscar.br (B.C. Janegitz).

<https://doi.org/10.1016/j.snr.2022.100118>

Received 13 July 2022; Received in revised form 15 August 2022; Accepted 19 August 2022

Available online 30 August 2022

2666-0539/© 2022 The Author(s). Published by Elsevier B.V. This is an open access article under the CC BY-NC-ND license (<http://creativecommons.org/licenses/by-nc-nd/4.0/>).

explore renewable and environmentally friendly substrates, such as paper [12]. In the view of green chemistry, the use of recyclable materials is very attractive. For example, Andreotti et al. [13] published an interesting work reporting the use of PET sheets obtained from discarded soda bottles as the substrate for graphite conductive ink. In this regard, PET bottle substrates have been attractive due to their easy accessibility, and relative flexibility, which can be ideal for the construction of wearable sensors for example.

The analysis of clinically relevant molecules assists the understanding of biological and physiological functions in the human body, which can be used as biomarkers for the diagnosis of diseases. In this aspect, glucose and uric acid (UA) are two relevant examples [14]. Glucose biosensors are important platforms for the diagnosis of diabetes mellitus, which directly affects the quality of life of the patients. On the other hand, glucose monitoring can be performed in a non-invasive way, with no need for blood samplings, such as sweat, tears, and interstitial fluid [15,16]. Therefore, the detection of glucose in sweat samples can be viable by employing wearable sensors. Electrochemical detection of glucose can be accomplished by the enzyme glucose oxidase (GOx), which acts in the oxidation of glucose and reduction of O_2 , producing hydrogen peroxide, a by-product generated during the enzymatic reaction [14]. Nevertheless, other mediators can be also employed, and a combination of such compounds can improve the analysis. Prussian blue (PB), also known as ferric hexacyanoferrate, is widely used in the development of (bio)sensors [17]. Its high effectiveness in hydrogen peroxide reduction makes this material largely used for the construction of glucose biosensors, and improvements in the sensitivity of the analysis can be obtained due to its excellent electrocatalytic properties [18]. Furthermore, the levels of UA in the human body and the risk of diabetes, are correlated. Studies indicate that high levels of UA are directly associated with an increased risk of diabetes [19,20]. UA is considered an end product of purine metabolism and is generally a predictor of several diseases such as hypertension, chronic renal disease, and metabolic syndrome [21].

Thus, herein we propose the use of a disposable, environmentally friendly PB-modified electrochemical (bio)sensor, employing recyclable PET bottle substrate and a simple conductive ink based on NP and graphite, for the enzymatic detection of glucose and non-enzymatic detection of UA and hydrogen peroxide in synthetic sweat samples. Also, to present the possibility to employ the proposed platform as a wearable sensor, a wristband was constructed using the 3D printing technology and tested facing UA response, showing the versatility of the proposed sensor.

2. Experimental

2.1. Reagents and solutions

All reagents used in this work were of analytical grade. Ultrapure water (Milli Q, USA), with resistivity $> 18 \text{ M}\Omega \text{ cm}$, was used to prepare all the aqueous solutions. Graphite from Fisher Chemical™ (New Jersey, USA) and colorless NP(Base brilho cuidados, Cora ©, São Paulo, Brazil) were used for the preparation of the conductive ink. UA (99% w/w), ferrocene methanol (FcMeOH - 97% w/w), potassium chloride ($\geq 99\%$ w/w), hydrogen peroxide (H_2O_2 - 35% v/v), glucose (99.5% w/w), dopamine hydrochloride (99% w/w), and GOx were purchased from Sigma-Aldrich®, USA. Ascorbic acid (99% w/w) from Dinamica, Brazil; fructose ($\geq 99\%$ w/w) from Synth®, Brazil and sucrose (99% w/w) from Vetec®, Brazil were also used in this work. Stock solutions of UA (5.0 mmol L^{-1}) were freshly prepared before the experiments, after dissolution in 0.01 mol L^{-1} sodium hydroxide (98% w/w from Dinamica®, Brazil). The electrochemical characterization of the electrodes was performed using a 1.0 mmol L^{-1} FcMeOH solution in 0.1 mol L^{-1} KCl. For the detection of UA, hydrogen peroxide, and glucose, 0.1 mol L^{-1} phosphate buffer saline solution (PBS) (pH 7.0) was used as the supporting electrolyte. Synthetic sweat was produced with NaCl (99% w/w

- Vetec®, Brazil), urea (99% w/w) and acetic acid (99.7% v/v), lactic acid (85% v/v), and ammonium chloride (99.5% w/w) from Dinamica® (Brazil), UA, and glucose from Sigma-Aldrich®, USA. The flexible and non-conductive acrylonitrile butadiene styrene (ABS) filament, used in the construction of a wearable wristband, was purchased from 3DLAB (Minas Gerais, Brazil).

2.2. Apparatus

Electrochemical analyses were performed using the AUTOLAB 204 potentiostat/galvanostat. The instrument was coupled to a computer and controlled by NOVA 2.1 software. The conductive ink was mixed and milled with a dual asymmetric centrifuge (DAC) SpeedMixer™ Dac 150.1 FVZ-K (FlackTec Inc) and the electrodes were cut with a cutting printer (Silhouette, Cameo 3). Fourier transform infrared spectroscopy (FTIR) was carried out with a Tensor II spectrophotometer (Bruker). Scanning electron microscopy (SEM) from Thermo Fisher Scientific model Prisma E with ColorSEM Technology and integrated energy-dispersive X-ray spectroscopy was used for the acquirement of SEM images. For comparison of the surface morphology, a commercial carbon-based screen-printed electrode from MicruX technologies was analyzed by SEM. A 3D printed wearable wristband was designed in the free Blender software version 2.91.2 and manufactured with a Sethi3D S3 3D printer by using ABS.

A three-electrode system configuration, based on the design of a commercial screen-printed electrode, was used for the construction of the disposable electrodes. The proposed working electrode consisted of a circle of 4.95 mm in diameter (geometric area of 0.19 cm^2). All three electrodes were composed of the conductive ink proposed (described in Section 2.3), and further modified with PB. This platform was directly employed for hydrogen peroxide and uric acid detection, and the construction of the glucose biosensor by anchoring GOx.

2.3. Manufacture of the disposable electrodes

Firstly, the PET bottle substrates were sanded with conventional sandpaper ($n^\circ. 220$ from 3M™) to facilitate the deposition of the ink on the substrates. The substrate was then cleaned with ethanol (70% v/v) to remove organic residues/impurities that might interfere with the electrochemical analysis, as exemplified in step 1 (Fig. 1). Masks cut from adhesive paper (Colacril, Office CC185) were used for delimiting the electrodes and giving their shape. For that, a cutting printer was used, with designs being created with the Silhouette Studio software version 4.4. The inner part of the structures was removed and then the masks were glued on the surface of a PET sheet obtained from a discarded soda bottle. The conductive ink was prepared by mixing NP and graphite (48:52% (w/w)) (Fig. 1, step 2), a composition previously optimized by de Araujo Andreotti et al. [13]. The prepared ink was deposited and spread evenly on the masks, as shown in step 3 (Fig. 1). The produced graphite-nail polish-based electrode was named GNP.

2.3.1. Prussian blue electrodeposition

The modification of the electrodes was performed by electrodeposition of a PB film (step 4, Fig. 1), providing the GNP/PB electrodes. The electrodeposition of PB was based on methods described in the literature [22] and involved consecutive cycling ($n = 15$) employing the cyclic voltammetry (CV) technique in potentials ranging from -0.3 to 0.8 V at 50 mV s^{-1} in an aqueous solution of $2.5 \text{ mmol L}^{-1} \text{ K}_3[\text{Fe}(\text{CN})_6]$ containing $2.5 \text{ mmol L}^{-1} \text{ FeCl}_3$, in $0.1 \text{ mol L}^{-1} \text{ KCl}$ (pH 3.0) acidified with $0.1 \text{ mol L}^{-1} \text{ HCl}$. A time-lapsed video is available and shows the complete manufacturing process of GNP/PB.

2.3.2. Biosensor fabrication

For the fabrication of the biosensor (step 5, Fig. 1), $50 \mu\text{L}$ of a 0.2% chitosan (CS) biopolymer dispersion was mixed with $50 \mu\text{L}$ of 2% glutaraldehyde solution. The mixture was left to stand for 30 min for the

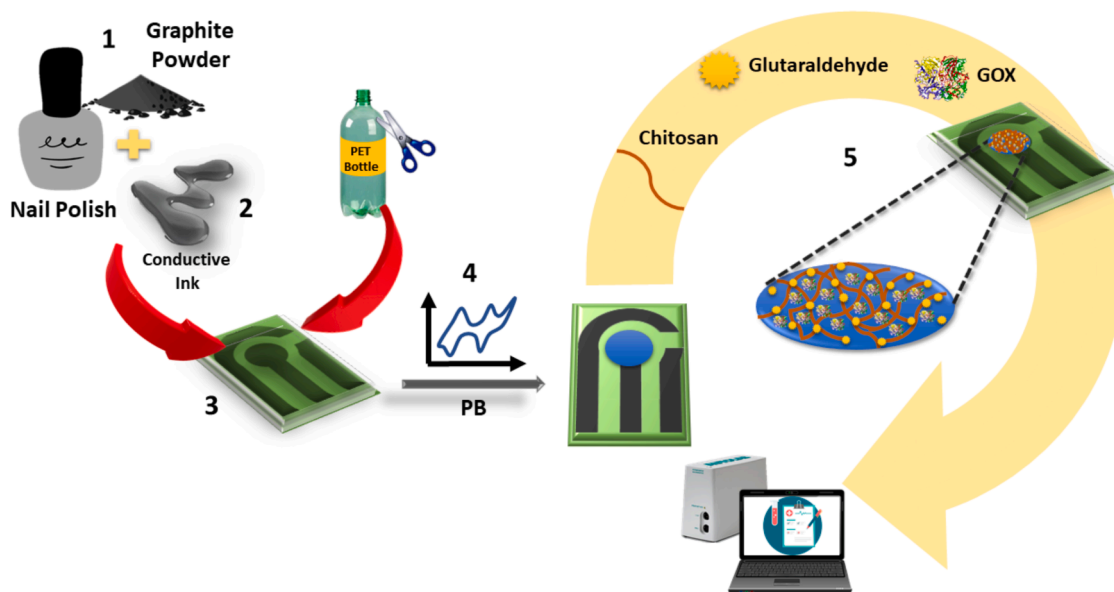


Fig. 1. Preparation of GNP and GNP/PB electrode: (1 and 2) Preparation of the conductive ink. (3) Application of conductive ink and GNP electrode. (4) Electrodeposition of PB film and GNP/PB electrode. (5) Preparation of the GNP/PB/GOx biosensor.

two aldehyde groups of the glutaraldehyde to interact completely with the NH_2 groups of the CS. Thus, a crosslinked matrix with the enzyme GOx imprisoned between the interstices is formed [23]. Then, 50 μL of a 30 mg mL^{-1} GOx solution was added to the mixture. This covalent

bonding method provided better biocompatibility and stability for the enzyme. Finally, 7 μL of the final mixture was added to the working electrode surface and left to dry overnight at 10 $^\circ\text{C}$. The biosensor was named GNP/PB/GOx.

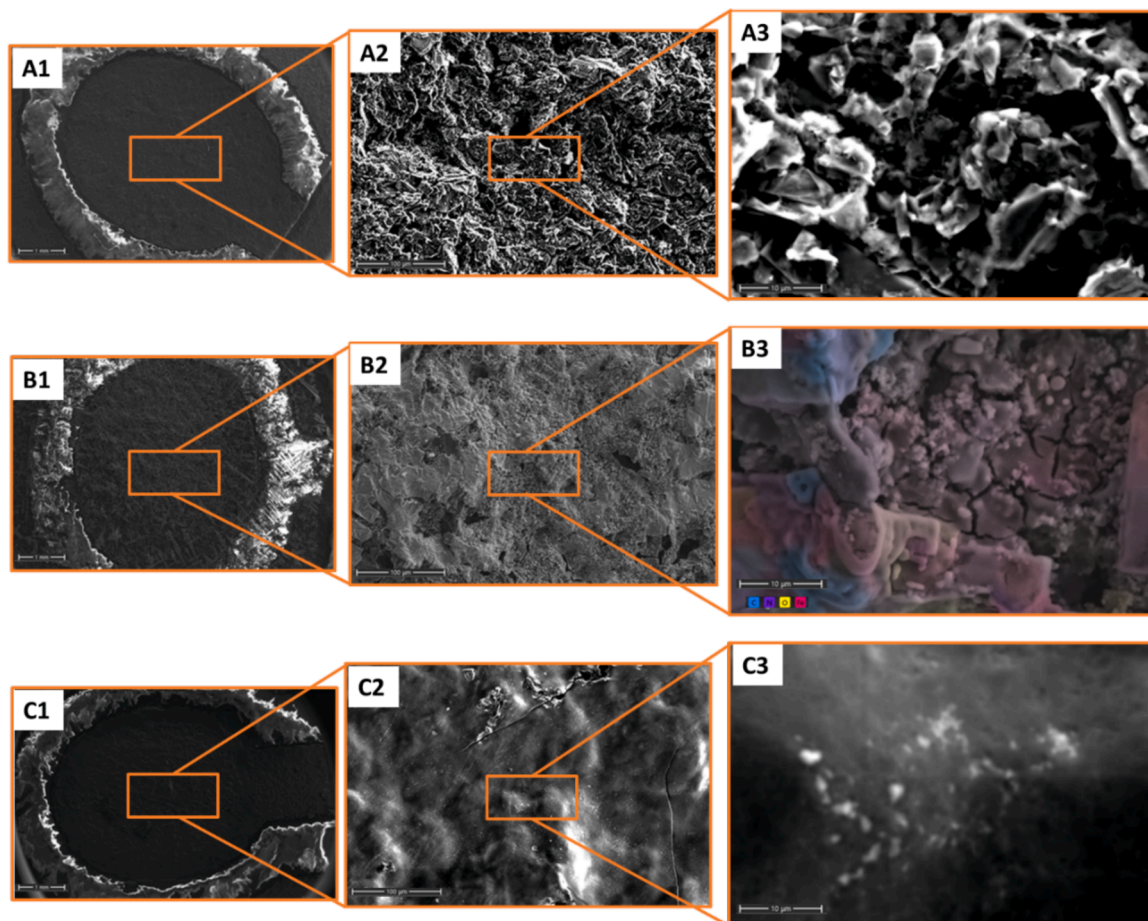


Fig. 2. SEM images of (A) GNP, (B) GNP/PB e (C) GNP/PB/GOx after 60 (1) 1000 (2) and 8000 (3) amplification factors. Color SEM with the distribution of the chemical elements on the surface of the electrode (B3) GNP/PB.

2.4. Analytical procedure and samples analyses

CV experiments were performed to characterize electrochemically the obtained sensor, and evaluate the electrochemical behavior of the molecules. UA detection was performed using the DPV technique, employing optimized operational parameters (modulation amplitude: 80 mV; modulation time: 5 ms; step potential: 7 mV s⁻¹). H₂O₂ and glucose detection were performed employing the amperometry technique, by applying a constant and optimized working potential of -0.3 V during 120 ms. All measurements were performed using 0.1 mol L⁻¹ PBS solution (pH 7.0) as a supporting electrolyte. Synthetic sweat samples were prepared according to the suggested chemical formulation proposed in the literature [24] and subsequently spiked with UA or glucose in different concentrations. For UA analysis, synthetic sweat was spiked with 4 different UA concentrations (5.0, 20.0, 40.0, and 59.0 μmol L⁻¹) and for glucose detection, the fortification involved 3 different concentrations (50.0, 150.0, and 400.0 μmol L⁻¹). All fortifications were performed in concentrations within the linear working range.

3. Results and discussion

3.1. Morphological and electrochemical characterization of the disposable device

The morphologies of the electrodes based on graphite conductive ink before and after modification with PB, and of the modified electrode containing GOx were characterized by SEM, and the obtained images are shown in Fig. 2A, 2B, and 2C, respectively. Through the SEM images presented in Fig. 2-A2 and A3 is possible to observe graphite sheets distributed homogeneously all over the electrode surface. In addition, a rough and porous topography with the presence of cavities is observed. Such cavities are interesting for electroanalysis since they can provide active sites capable of performing the interaction and immobilization of species, such as some electrochemical mediators, thus enhancing the conductivity of the device. For comparison, SEM images were also obtained for a commercial screen-printed carbon electrode applying the same amplification factors, and the images are presented in Fig. S1. As can be seen, the surface of a commercial electrode is significantly smoother than GNP, confirming that GNP presents more sites and cavities, and a considerable rough surface, adequate for the anchoring of species. After modification with PB (Fig. 2-B2), the electrode surface was covered homogeneously by the PB film. This fact is evidenced by the presence of iron confirmed by the energy dispersive spectroscopy image that provides the color SEM (Fig. 2-B3) and the respective spectrum, shown in Fig. S2. The red coloration from Fig. 2-B3 indicates the

presence of Fe, while the blue coloration indicates the presence of C, confirming the successful synthesis of PB, and the percentage corresponding to each element found is presented in Table S1. In addition, small cracks can be seen, which shows that the nucleation process for the growth and formation of the PB film occurred effectively. Finally, SEM images from the biosensor containing GOx (Fig. 2C) show a smoother surface with the presence of small clusters related to the film GNP/PB/GOx.

The FTIR spectra were obtained for GNP and GNP/PB electrodes to observe their surface composition and possible changes after the surface modification. The obtained spectra are presented in Fig. 3A. It is possible to observe that for GNP there are predominant bands in the region between 1800 and 800 cm⁻¹, in which oxygenated groups are assigned, such as carboxyl and/or carbonyl (1717 and 1445 cm⁻¹) [25]. In this regard, the bands at 1222 and 1113 cm⁻¹, can be related to the C-O-C stretching vibration [25]. These bands can be attributed to compounds present in the NP, such as toluene, isopropyl alcohol, butyl acetate, and formaldehyde resin, among others, used in the manufacture of conductive inks. On the other hand, in GNP/PB spectra, a high-intensity band at 2070 cm⁻¹ can be observed. This band is related to C≡N functional groups and originated from PB. These results corroborate that the modification of the disposable sensor with PB was successful.

After physicochemical surface characterization, electrochemical characterizations were performed using CV to study the electrochemical behavior of the GNP/PB electrode. Fig. 3B shows the voltammograms obtained for GNP (black line) and GNP/PB (red line) and the respective redox pair.

It can be seen from the CVs that no redox processes are involved in the supporting electrolyte employing the GNP electrode. After electro-deposition of the PB film (red line), the typical redox processes indicating the presence of PB are present, composed of two oxidation and two reduction peaks. The first redox signal (I) is an oxidation peak at around +0.04 V attributed to PB. The oxidation of PB provides a peak at around +0.76 V, related to Berlin green (III), and oxidated form of PB. The subsequent reduction of Berlin green provides PB at around +0.52 V, and a second reduction process generates Prussian white (IV) at -0.25 V. These processes are well described in the literature [26] and confirm the synthesis of PB on the electrode surface.

The electroactive area of GNP and GNP/PB was also calculated. For this, cyclic voltammetric studies were performed at different scan rates (30, 50, 70, 90, 110, 130, 160, 200, and 250 mV s⁻¹) at both electrodes (Fig. S3). The electroactive area was calculated based on the Randles-Sevcik equation (Eq. (1)), using a 1.0 mmol L⁻¹ FcMeOH solution in 0.1 mol L⁻¹ KCl:

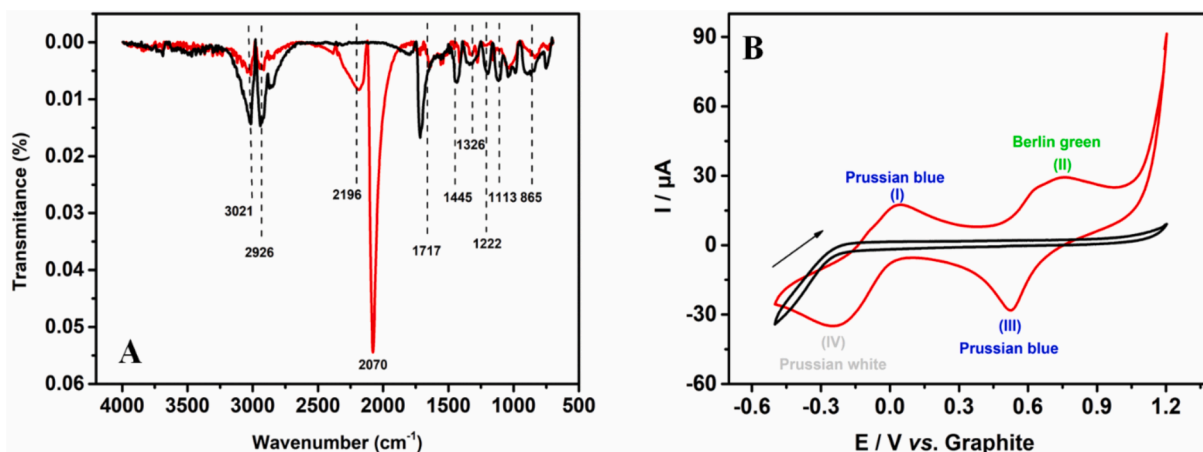


Fig. 3. (A) FTIR spectra for GNP (black line) and GNP/PB (red line); (B) Cyclic voltammograms in absence (black line) and presence (red line) of Prussian blue in 0.1 mol L⁻¹ PBS solution (pH = 7.0); Scan rate: 50 mV s⁻¹.

$$I_p = 2.69 \times 10^5 ACD^{1/2}n^{3/2}v^{1/2} \quad (1)$$

where, I_p is the peak current (A), A the electroactive area (cm^2), C the concentration of the redox probe (mol L^{-1}), D the diffusion coefficient of the redox probe ($\text{cm}^2 \text{s}^{-1}$), n the number of electrons involved in the reaction, and v the scan rate (mV s^{-1}). The diffusion coefficient used for FcMeOH was $7.6 \times 10^{-6} \text{ cm}^2 \text{s}^{-1}$, following studies previously reported in the literature [27].

The values obtained were 0.16 and 0.95 cm^2 for GNP and GNP/PB, respectively. Firstly, it is noteworthy to mention that the geometric area of the electrode is slightly higher (0.19 cm^2) than the electroactive surface area of unmodified GNP. This occurs due to the composition of the electrode (conductive ink), which presents non-conductive NP in its composition, thus, only parts of the electrode surface are electroactive and responsible for the electron transfer process. When comparing the electroactive area of unmodified and PB-modified electrodes, it can be seen that there is an increase of approximately 6-fold in the electroactive area after PB modification. Such an increase probably occurred due to the rise of the surface roughness of the material after PB deposition, where cracks in the surface were observed through SEM images. This increase in electroactive area is beneficial for the adsorption of analytes and the immobilization of enzymes, increasing the electrochemical response and decreasing the detectability [28].

The inset curves in Fig. S3, related to the plot of peak current *versus* square root of scan ($v^{1/2}$), show a linear behavior for both surfaces with linear responses of $R^2 = 0.9955$ (GNP) and $R^2 = 0.9986$ (GNP/PB), following the equations: $I_p (\mu\text{A}) = -5.251 \times 10^{-6} + 1.228 \times 10^{-4} C_{\text{FcMeOH}} (\mu\text{mol L}^{-1})$ and $y = -5.024 \times 10^{-5} + 7.158 \times 10^{-4} C_{\text{FcMeOH}} (\mu\text{mol L}^{-1})$, respectively, that indicates that at both electrodes the mass transport processes are diffusion-controlled [29].

3.2. Electrochemical detection of UA

After characterizing the electrodes, these were evaluated regarding the detection of UA. The electrochemical performance of the sensor toward the detection of UA was initially evaluated by CV in a 0.1 mol L^{-1} PBS solution (pH 7.0) in the presence of $800.0 \mu\text{mol L}^{-1}$ UA at a scan rate of 50 mV s^{-1} . Fig. 4A presents the obtained voltammograms for GNP in presence of UA (blue line), and GNP/PB in the presence (red line) and absence (black line) of UA. It is possible to observe that UA presents a well-defined oxidation peak at around $+225 \text{ mV}$ at GNP/PB. In presence of PB (red line), though the typical peaks related to the redox

processes of PB are decreased, it can be seen that the oxidation process of UA is improved, presenting a higher peak current value corresponding to an increase of 43%. This result is in agreement with the electroactive area values calculated, where an increased area is observed for GNP/PB. Thus, this surface provides more electroactive sites for the oxidation of UA and greater peak currents are observed. In addition, the oxidation occurred in decreased working potential ($+250 \text{ mV}$), which can indicate that PB film catalyzed the reaction, which increases the electrochemical performance of the device. Furthermore, no interferences of the redox processes of PB are occurring, indicating that GNP/PB has a great potential in the sensing of UA, thus being an interesting material to be employed.

Different voltammetric techniques were tested to evaluate UA electrochemical response. Fig. S4 presents the voltammograms obtained for $50.0 \mu\text{mol L}^{-1}$ UA using differential pulse voltammetry (DPV) and square wave voltammetry (SWV) techniques, considering the maintenance of the scan rate (10 mV s^{-1}) at both techniques for a better comparison. A higher peak current value was obtained by DPV (14-fold higher), indicating that DPV is more adequate for the determination of UA. Thus, this technique was employed for further tests involving UA determination.

After the selection of the technique, the optimization of DPV operational parameters (modulation amplitude, modulation time, and step potential) was performed to guarantee the best electrochemical response. For this, a univariate study was performed at a solution containing $50.0 \mu\text{mol L}^{-1}$ UA keeping two parameters fixed while the third one was varied. For this study, the DPV parameters were fixed as follows: modulation time (mt): 25 ms ; modulation amplitude (a): 50 mV ; and step potential (ΔE): 5 mV . The voltammograms obtained are presented in Fig. S5, as well as the corresponding plots of the current response. We observed that the increase in the step potential values lead to an increase in the current response, and a step potential of 7 mV was chosen for further experiments since, for higher values, an increase in the peak width was observed, as well as the increase in the baseline noise magnitude (Fig. S5-A). The same increase in the current response was observed for amplitude variation, where a maximum in the current response is reached at 80 mV of amplitude (Fig. S5-B). Therefore, this value was selected as optimum. It can also be seen that increases in the modulation time reduce the peak current of UA (Fig. S5-C), and since higher electrochemical responses are aimed, a low modulation time value (5 ms) was chosen as optimum for further DPV experiments.

Under optimized conditions, a calibration curve was obtained for

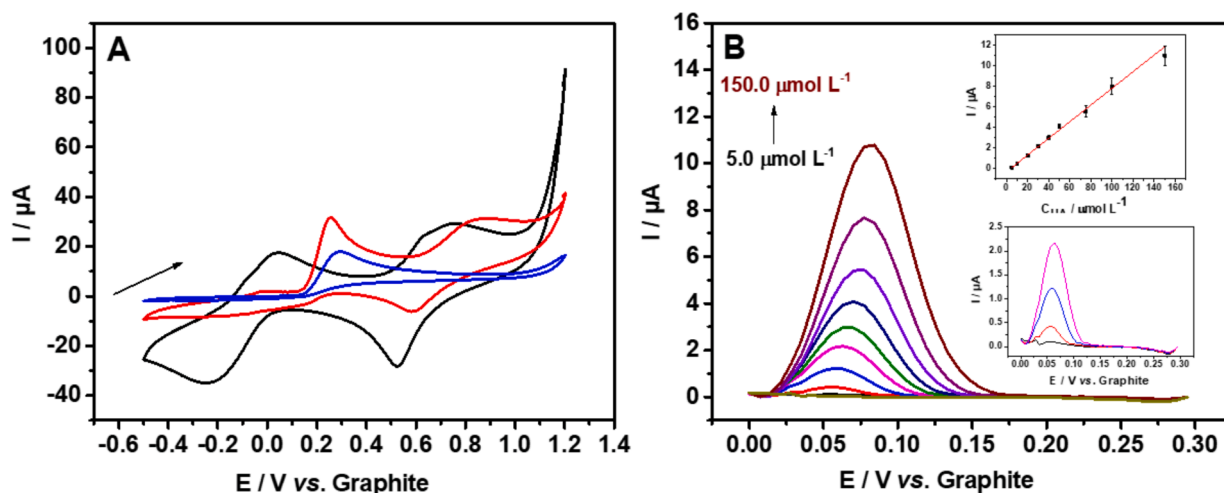


Fig. 4. (A) Cyclic voltammograms obtained for GNP (blue line) in presence of $800 \mu\text{mol L}^{-1}$ UA, and for GNP/PB in the absence (black line) and presence (red line) in presence of $800.0 \mu\text{mol L}^{-1}$ UA, in 0.1 mol L^{-1} PBS solution (pH 7.0); (B) Differential pulse voltammogram obtained in 0.1 mol L^{-1} PBS solution (pH 7.0) at different concentrations of UA from 5.0 to $150.0 \mu\text{mol L}^{-1}$; Inset: Plot of peak current *versus* uric acid concentration. Experimental conditions DPV: modulation amplitude: 80 mV ; modulation time: 5 ms ; step potential: 7 mV s^{-1} .

increasing concentrations of UA (Fig. 4B). A linear behavior was obtained at a concentration range varying from 5.0 to 150.0 $\mu\text{mol L}^{-1}$, as observed in the inset curve (Fig. 4B), following the equation: $I_p (\mu\text{A}) = -2.981 \times 10^{-7} + 8.079 \times 10^{-8} C_{\text{UA}} (\mu\text{mol L}^{-1})$, with R^2 of 0.990. The limits of detection (LOD) and quantification (LOQ) were calculated according to 3 and 10 times the intercept standard deviation over the analytical sensitivity of the calibration curve [30,31]. The values of LOD and LOQ obtained were 0.70 and 2.50 $\mu\text{mol L}^{-1}$, respectively, indicating that GNP/PB presents the potential for the detection of UA in a wide linear working range and low concentrations. For evaluating the precision of the sensor, a repeatability study was performed by performing 20 consecutive DPV measurements at the same sensor. Fig. S6 shows the voltammograms and the respective plot of peak current in the function of repetition number. As can be seen, and according to the RSD obtained (4.72%), the proposed sensor presented satisfactory precision and can be applied for consecutive measurements with no performance loss. In addition, an inter-electrode tests were performed to evaluate the reproducibility of the obtained sensors. For this, five different sensors were evaluated by performing DPV measurements in a solution containing 25.0 $\mu\text{mol L}^{-1}$ UA, and the voltammograms are presented in Fig. S7. A low RSD value was obtained (3.59%), indicating that the construction of the sensors is reproducible. Finally, the stability of the sensors was also evaluated. Fig. S8-A shows consecutive DPV measurements ($n = 40$), recorded in a solution containing 25.0 $\mu\text{mol L}^{-1}$ UA, and Fig. S8-B the respective current response. As can be seen, a decrease of 2.7% in the current response is observed after 5 measurements. After 10 scans, a decrease of 4.3% is observed, while after 20 scans, 7.9% of the current response is observed, indicating a loss in the stability of the sensor. In this sense, each sensor can be used for about 20 measurements without loss in stability. Thus, a satisfactory performance can be observed, allowing several analyses. Also, considering that the proposed sensor is disposable and of easy obtention, when the sensor loses stability, an easy replacement is possible.

The proposed disposable electrode was compared to other already reported electrochemical devices for the detection of UA [32–37], as presented in Table S2. In this regard, Guan et al. [34] presented a sensor for UA determination using amino-functionalized carbon nanotubes and gold nanoparticles. The authors obtained a LOD of 0.29 $\mu\text{mol L}^{-1}$ with a linear range of 0.3 to 200.0 $\mu\text{mol L}^{-1}$. Although the sensor proposed by the authors presented a slightly lower LOD, the synthesis of materials and assembly of the sensor requires more than 3 days. In contrast, our proposed sensor takes approximately 1.5 days between the preparation steps of the PET substrate, conductive ink, and modification with PB. Yang et al. [36] on the other hand, simultaneously determined UA, dopamine (DA), and ascorbic (AA) acid using a reduced graphene-modified electrode. The determination was carried out by surface the modification of a glassy carbon electrode (GCE) with graphene, and a linear response was obtained in a range of 0.5 to 60.0 $\mu\text{mol L}^{-1}$, with a LOD of 0.5 $\mu\text{mol L}^{-1}$. After that, Xu et al. [35], also proposed a modified GCE, for the simultaneous determination of DA and UA in the presence of AA. In this work, the authors employed reduced graphene oxide Pt nanoparticles as modifiers. A linear range of 10.0 to 100.0 $\mu\text{mol L}^{-1}$ was achieved, with a LOD of 0.45 $\mu\text{mol L}^{-1}$. Although the authors reported a low LOD, time-consuming procedures were required to produce the sensors and, in addition, the use of GCE restricts the application of the device as a wearable sensor.

It has been reported that UA can be found in human sweat in concentrations ranging from 24.5 to 35.7 $\mu\text{mol L}^{-1}$ [38], which confirms the adequacy of the proposed sensor for clinical analysis. For evaluating the performance of the proposed device in complex media, the detection of UA was performed in synthetic sweat samples. For this, a recovery test was performed after the fortification of the sample with four different UA concentrations (5.0, 20.0, 40.0, and 59.0 $\mu\text{mol L}^{-1}$), and the obtained results are presented in Table S3. From the table, it can be seen that recovery values ranging from 102.3% \pm 3.4 to 113.0% \pm 1.8 were obtained, indicating that no interferences from the sample matrix are

present. Thus, GNP/PB can be successfully applied in the detection of UA, being an interesting alternative to conventional electrodes.

3.3. Sensing of H_2O_2

Hydrogen peroxide is a product obtained during the enzymatic reaction between glucose and GOx [39]. In this sense, previous to the construction of the glucose biosensor, GNP/PB was tested for the detection of H_2O_2 .

The detection of H_2O_2 was performed using the amperometric technique and current values were collected after 120 s of measurements. Initially, a hydrodynamic potential study evaluated the best working potential to be applied. Triplicate amperometric recordings (120 s) for 400.0 $\mu\text{mol L}^{-1}$ H_2O_2 in 0.1 mol L^{-1} PBS solution (pH 7.0) were obtained for each studied potential (from -0.5 V to 0.0 V) using GNP/PB electrodes. Fig. 5A shows the current response for each studied potential, where ΔI corresponds to the current response of H_2O_2 subtracted from the background current (supporting electrolyte) at the respective applied potential. It is possible to observe that at more negative potentials, higher than -0.1 V, a significant increase in the current response is obtained, reaching a maximum value at the potential of -0.3 V, with no significative changes after that. Considering that -0.3 V provided the best current response and that, at high potentials, the interference of other compounds is more present, this value was employed for further experiments. In addition, this working potential is close to the one used in the literature [40].

As a proof-of-concept, the determination of H_2O_2 was performed employing the GNP/PB electrode. In this regard, amperometric recordings were obtained for increasing concentrations of H_2O_2 ($n = 3$) at GNP (Fig. 5B) and GNP/PB (Fig. 5C) electrodes. As can be seen, in absence of PB (Fig. 5B), no electrochemical response is observed for hydrogen peroxide, even at high concentrations (5.0 mmol L^{-1}). This behavior is expected since this reaction needs to be catalyzed to occur. As can be seen in Fig. 5C, the presence of PB is of great importance, since allows the detection of hydrogen peroxide. For increasing concentrations of hydrogen peroxide, a linear behavior was obtained at concentrations ranging from 100.0 to 800.0 $\mu\text{mol L}^{-1}$ (Fig. 5D). The respective calibration curve follows the equation $I_p (\mu\text{A}) = 6.828 \times 10^{-7} + 1.241 \times 10^{-8} C_{\text{H}_2\text{O}_2} (\mu\text{mol L}^{-1})$, with R^2 of 0.996. The LOD and LOQ values were calculated using the same equation as proposed previously and the values obtained were 31.6 $\mu\text{mol L}^{-1}$ and 100.0 $\mu\text{mol L}^{-1}$, respectively.

Thus, it can be seen that the determination of H_2O_2 can be performed employing the proposed sensor modified with PB, allowing a fast, and simple analysis of this compound. The detection of H_2O_2 is of great interest since it allows a great range of applications, either for the indirect detection of biomarkers such as glucose cholesterol or lactic acid. Since this compound is a byproduct of enzymatic reactions, it is involved in these biological processes [41] and allows the development of alternative sensors for clinical analysis of some diseases such as cholesterol and cancer, Alzheimer's, and Huntington's [42]. Therefore, its facility of confection and excellent analytical characteristics are comparable or superior to those observed, as presented in Table S4 [43–47], attesting that the proposed sensor can be successfully employed for clinical analysis.

3.4. Glucose biosensor

After showing that PB/GNP provides a satisfactory response for hydrogen peroxide, an enzymatic glucose biosensor was developed onto the GNP/PB surface. In this context, the immobilization of GOx by covalent bonding was performed [48], which has the advantage of bypassing the desorption phenomenon, and thus affecting the performance of the biosensor. For the construction of the biosensor, the concentration of CS (0.2%, 0.4%, and 0.6%) was evaluated for the immobilization of GOx at the electrode surface with a fixed amount of

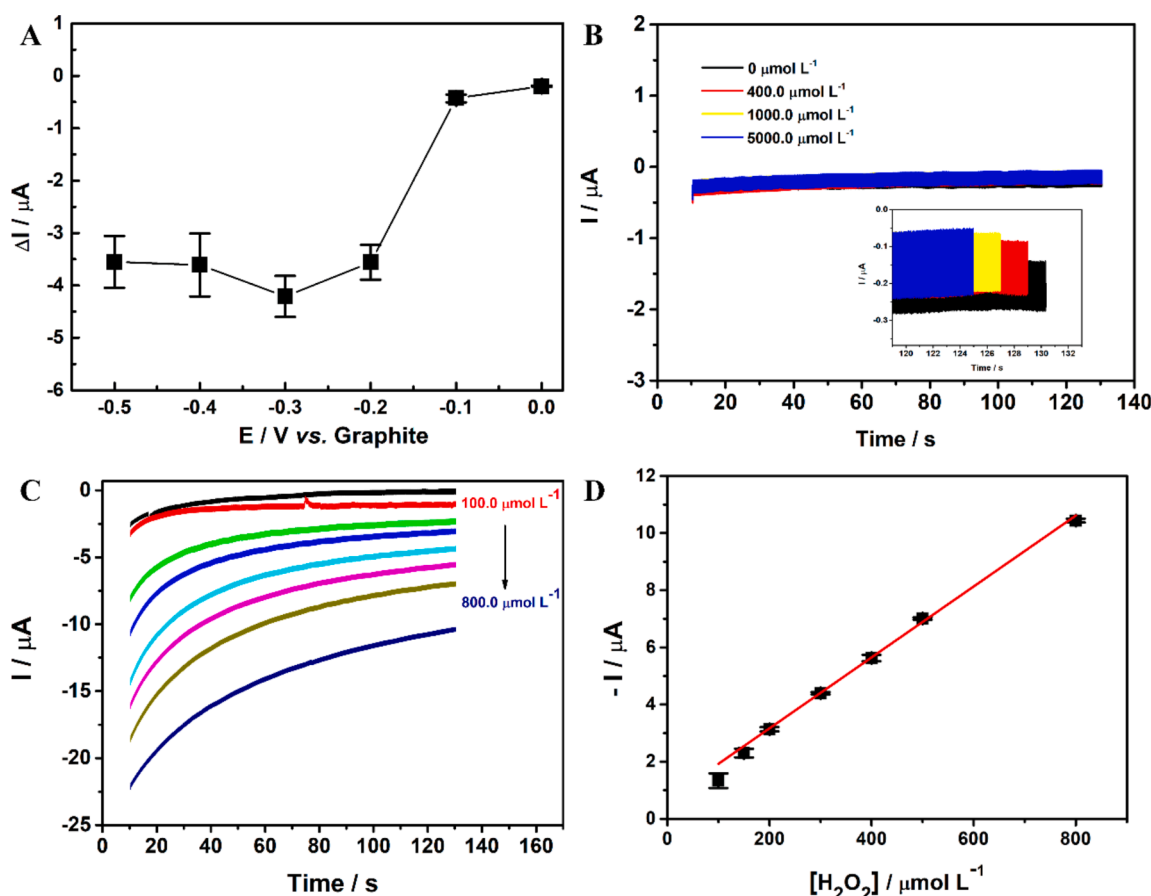


Fig. 5. (A) Hydrodynamic potential study for $400.0 \mu\text{mol L}^{-1}$ hydrogen peroxide using GNP/PB electrode obtained after amperometric measurements (duration of 120 s; $n = 3$) in varied working potentials; (B) Amperometric recordings for increasing concentrations of hydrogen peroxide ($0.0, 400.0, 1000.0$ and $5000.0 \mu\text{mol L}^{-1}$) at GNP, working potential: -0.3 V (120 ms); (C) Amperometric recordings for increasing concentrations of hydrogen peroxide (100.0 to $800.0 \mu\text{mol L}^{-1}$) at GNP/PB, working potential: -0.3 V (120 ms); (D) Plot of peak current versus hydrogen peroxide concentration, obtained from C.

2% glutaraldehyde solution. It was observed that with CS concentrations higher than 0.2%, a poor signal response was obtained with the transducer (Fig. S9). This is directly related to the low conductivity of CS, which can affect the performance of biosensors [49]. The concentration of glutaraldehyde used in this work was fixed at 2%, based on previous studies from the literature [50].

After the concentrations of CS and glutaraldehyde were established, the electrochemical behavior of glucose was evaluated using the proposed biosensor. All the analyses were performed at pH 7.0, once acid solutions can affect the enzyme activity, and high alkaline media cause a decrease in the stability of PB film, in addition to impairing the GOx activity [51]. Therefore, CVs were recorded using a 0.1 mol L^{-1} PBS

solution (pH 7.0). Fig. 6A shows the voltammograms obtained at GNP/PB/GOx in the presence and absence of glucose.

The redox process of PB can be noticed at the studied potential window both in the presence and absence of glucose, however, when glucose is present, a reduction peak is observed at a potential of -0.3 V, attesting that the proposed biosensor is capable of detecting glucose. For the development of the detection method employing amperometry, a hydrodynamic study was also performed for glucose, as performed for H_2O_2 sensing. Fig. S10 presents the obtained current responses for different applied potentials (ranging from 0.0 to -0.4 V). A higher current response was obtained at -0.3 V. This result is in agreement with the proposed sensor for hydrogen peroxide (Fig. 5A) since the

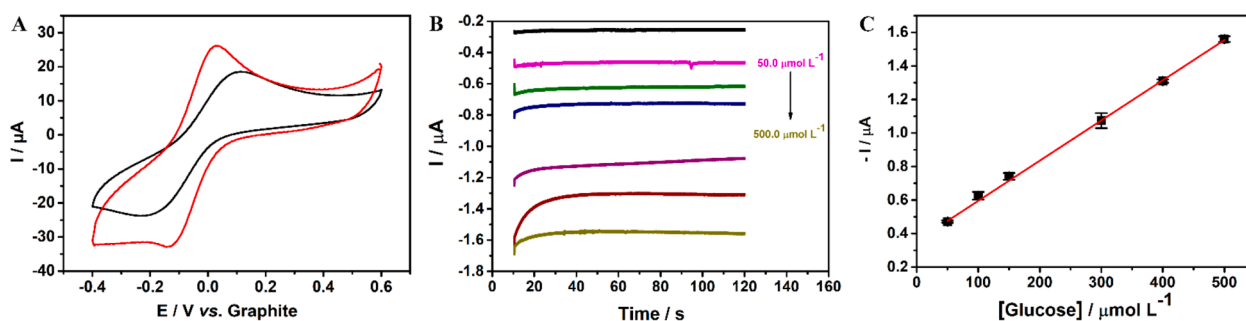


Fig. 6. (A) Cyclic voltammograms in the absence (red line) and presence (black line) of glucose using the GNP/PB/GOx; (B) Amperometric recordings for increasing concentrations of glucose (50.0 to $500.0 \mu\text{mol L}^{-1}$) in 0.1 mol L^{-1} PBS (pH 7) containing 0.1 mol L^{-1} KCl solution at GNP/PB/GOx, working potential: -0.3 V (120 ms); (C) Plot of peak current versus glucose concentration, obtained from C.

enzymatic detection of glucose generates hydrogen peroxide, which is indirectly detected by the biosensor. Thus, a behavior similar to the observed for hydrogen peroxide at GNP/PB was expected. Also, this value is also in agreement with the employed in the literature [52].

After the optimization of the working potential, a calibration curve was obtained for increasing concentrations of glucose employing the proposed biosensor (Fig. 6B). A linear behavior was observed with glucose concentrations ranging from 50.0 to 500.0 $\mu\text{mol L}^{-1}$ (Fig. 6C), following the equation $I_p (\mu\text{A}) = 3.554 \times 10^{-7} + 2.399 \times 10^{-9} C_{\text{glucose}} (\mu\text{mol L}^{-1})$, with the R^2 value of 0.999. The LOD and LOQ values were calculated as described for hydrogen peroxide, and the values were 9.2 and 30.6 $\mu\text{mol L}^{-1}$. The analytical performance of the biosensor was compared to other biosensors for the detection of glucose presented in the literature, and presented in Table 1.

GNP/PB/GOx has shown comparable or superior electrochemical performance to other biosensors for glucose detection and, in many cases, the proposed devices are of laborious obtention, and time-consuming, in contrast to the presented here. Also, the concentration of glucose in sweat samples is reported in the literature as ranging from 20.0 $\mu\text{mol L}^{-1}$ to 600.0 $\mu\text{mol L}^{-1}$ [60]. Thus, the proposed biosensor is adequate for sweat glucose analysis in most of the typical concentrations. To show the applicability of the proposed biosensor, recovery tests were performed by fortifying synthetic sweat samples with three different glucose concentrations (50.0, 150.0, and 400.0 $\mu\text{mol L}^{-1}$). The obtained results are presented in Table S5, and recovery values ranging from $91.56\% \pm 3.91$ to $100.5\% \pm 0.46$ were obtained, showing that GNP/PB/GOx can be successfully applied for the detection of sweat glucose. Repeatability and reproducibility studies were also performed to evaluate the performance of the proposed biosensor. For the repeatability study, ten successive amperograms were recorded (Fig. S11-A), under optimized conditions (working potential: -0.3 V , during 120 s), using a 150.0 $\mu\text{mol L}^{-1}$ glucose solution. An adequate result was obtained, with an RSD of 5.2%, indicating that for successive analysis, the

biosensor provided similar responses. This result can also indicate the stability of the biosensor, showing that after ten measurements, the biosensor still provided stable responses. For the reproducibility test, three different biosensors were evaluated by amperometric technique, using a 150.0 $\mu\text{mol L}^{-1}$ glucose solution, under optimized conditions (Fig. S11-B). The inter-electrode study showed the reproducibility in the manufacture of the biosensor since, from three different biosensors, the amperometric response provided a low RSD (1.37%).

Finally, a selectivity study was also performed. For this, different molecules, possibly found in conjunction with glucose in the human body, such as fructose, sucrose, ascorbic acid, uric acid, and dopamine, were evaluated in presence of glucose in two different ratios: 1:1 and 1:2 (glucose:interferent). The obtained amperograms and the respective current responses are presented in Fig. S12-A and B, respectively. The response of glucose individually (control) was evaluated. The current response of glucose in presence of the interferents was given in percentage, in which the positive values are attributed to an increase, and the negative values correspond to a decrease in the amperometric response of glucose. It can be observed that for a ratio of 1:1, most of the evaluated species are not interfering. A considerable interference from dopamine was observed, at approximately 53%, while ascorbic acid provided a slight interference in the glucose response, corresponding to 11.4%. When the proportion 1:2 (glucose:interferent) is evaluated, this behavior is accentuated for ascorbic acid, which provided an increase in the current response of around 3.65-fold, while dopamine increased the response by 1.48-fold. In this context, it has been shown that these molecules, especially in high concentrations when compared to glucose, are interfering in the glucose analysis when employing GNP/PB/GOx. In addition, uric acid becomes an interferent at higher concentrations, with an increase in the current response of 272.7%. These analytes have been previously reported in the literature as interfering species in glucose detection [61, 62]. Though selectivity has been an issue, some measures can be employed to circumvent this problem. The use of surface modifiers, which can increase the selectivity of the sensors can be an interesting option. In this sense, the literature reports the use of rhodium or ruthenium on carbon [63,64], metal complexes (cobalt phthalocyanine [65], metal porphyrin [66], and ruthenium complexes [67]), films based on electrostatic repulsion of the interferents such as Nafion [68].

In addition, the miniaturization, disposable use, easy preparation, and low-cost of the produced (bio)sensors, in conjunction with the satisfactory analytical performance, are attractive characteristics, making the proposed devices interesting tools to be applied for analysis *in loco*, allowing reliable analysis that can be employed for clinical analysis. The estimated cost per sensor unit considering only the materials employed was US\$ 0.004, and for the biosensor US\$ 0.42. An estimation including personnel and facilities costs, based on work from Brazaca et al. [69] which reported the values from the same region. It provides values of approximately US\$ 0.91 in the obtention of the sensor, and for each biosensor approximately US\$ 1.33, showing that these platforms are attractive in the face of laboratory testing. Thus, given the great performance of GNP/PB in sensing, and considering the versatility of the proposed sensor, the use of GNP/PB as a wearable sensor for the detection of UA was performed.

3.5. Application of GNP/PB as wearable sensor

Wearable sensors have received great attention in healthcare for monitoring clinical markers in biological fluids such as sweat, saliva, and tears [70,71]. Such platforms are devices that can be worn during physical activities to track the health and fitness of an individual, aiming for the real-time and continuous monitoring of relevant biomarkers. Furthermore, these platforms allow the substitution of conventional clinical diagnosis that demands expensive instrumentation, and large volumes of samples [71,72]. In this regard, 3D printing emerges as a great alternative to constructing wearable devices with interesting characteristics such as low-cost and the possibility to construct objects

Table 1

Analytical performance of the biosensor GNP/PB/GOx for glucose determination compared with the literature.

Electrode	Technique	Linear range ($\mu\text{mol L}^{-1}$)	LOD ($\mu\text{mol L}^{-1}$)	Ref
GOx/Chit/IL/PB/Pt	amperometry	10.0 to 4200.0	5.0	[53]
GOx/PB nanocubes	CV	10.0 to 1300.0	10.0	[54]
GOx/PPy/Al ₂ O ₃ /Pt	amperometry	500.0 to 1×10^4	30.0	[55]
rGO-GOx/PGE	amperometry	10.0 to 1000.0	5.8	[56]
GOx-DHP/Gr-AV	CV	1.0 to 10.0	0.21	[6]
Fe ₃ O ₄ @PNE-GOx	CV	200.0 to 2.4×10^4	6.1	[57]
GCE/Chi-Py/Au/GOx	amperometry	1000 to 2.0×10^4	68.0	[58]
CPE/GOx-SiO ₂ /Lig/Fc	amperometry	500.0 to 9000.0	145.0	[59]
GNP/PB/GOx	amperometry	50.0 to 500.0	9.2	This work

Notes: GOx/Chit/IL/PB/Pt: Pt electrode modified with PB, ionic liquid ([bmim]BF₄), chitosan and GOx; GOx/PB nanocubes: screen-printed electrode modified with nanocubic prussian blue crystals and glucose oxidase; GOx/PPy/Al₂O₃/Pt: biosensor based on polypyrrole (PPy) nanotube array deposited on a Pt plated nano-porous alumina substrate, modified with glucose oxidase; rGO-GOx/PGE: pencil graphite electrode modified with electrochemically reduced graphene oxide-glucose oxidase biocomposite; GOx-DHP/Gr-AV: conductive ink based on graphite and automotive varnish, modified with dihexadecyl phosphate and glucose oxidase; Fe₃O₄@PNE-GOx: nanoplateform based on polynorepinephrine grafted on magnetite nanoparticles with glucose oxidase; GCE/Chi-Py/Au/GOx: biosensor based on *in-situ* polypyrrole cross-linked chitosan/glucose oxidase/gold bionanocomposite film; CPE/GOx-SiO₂/Lig/Fc: carbon paste electrode based on functional glucose oxidase/silica-lignin system with ferrocene redox mediator.

with a great variety in composition and designs, enabling the obtention of non-invasive devices to be used in the monitoring of biomarkers in humans [73,74]. 3D printing technology can be a powerful tool for the obtention of objects on demand. The possibility to employ different materials and the molding of simple or more complex structures makes this technique a great option in the construction of wearable sensors [75]. Given that UA is a risk factor for diseases such as cardiovascular disease, renal disease, [76] and gout, the development of a wearable sensor for the detection of UA after the practice of physical activities is very attractive [76]. Thus, we propose the determination of UA employing the proposed GNP/PB sensor at a wearable wristband, obtained using 3D printing technology. The 3D printed wearable sensor was developed employing flexible non-conductive flexible ABS filament, and three conductive connectors were manufactured from homemade graphite and polylactic acid conductive filaments [77]. Fig. S13 shows the proposed wearable sensor, and the STL files for 3D printing are available on the journal website. A time-lapsed video is available showing the complete GNP/PB manufacturing process, including the obtention of the 3D printed wristband. As a proof-of-concept, measurements employing the produced wearable sensor were performed by DPV for UA.

The wristband allowed the electrochemical measurement of UA on synthetic sweat directly in contact with the skin. The electrochemical measurement was performed by adding 5 μL of a 100.0 $\mu\text{mol L}^{-1}$ UA solution, prepared in synthetic sweat, directly to a person's arm. For this, the wristband was placed with the electrode face directly to the sample, and a DPV measurement was then performed (Fig. S14). The obtained voltammogram was compared to the one obtained with the sensor not coupled to the wearable platform. Based on the measurements, it can be observed that a slight decrease in the current response occurred, however, this decrease corresponds to only 3%, indicating that the determination of UA can be performed directly towards the skin, with no prejudice to the electroanalytical response.

Considering that the amount of sweat excreted by a person during physical activities is 0.45 a 3.80 mL [78], the proposed wearable sensor is suitable for the analysis of an individual's sweat. It is also noteworthy to mention that if a portable potentiostat is employed, the analysis can be performed in loco right after exercising practice, or during physical activities, by the use of a miniaturized potentiostat and a software-controlled smartphone via wireless, allowing real-time analysis. The ability to be employed as a wearable sensor makes the proposed sensor a very interesting platform, and the possibility of monitoring UA levels during or shortly after physical activity plays an important role in the monitoring of physical conditions strictly related to several chronic health problems, ranging from heart disease, type 2 diabetes, and cancer [79]. Thus, the wearable device can act in health monitoring in a dynamic and non-invasive way.

4. Conclusion

This paper reports the development of a disposable (bio)sensor made of PET bottle substrate and low-cost conductive ink modified with PB film for the detection of UA, H_2O_2 , and glucose. The GNP/PB presented an excellent analytical performance for UA and hydrogen peroxide determination showing linear responses in a range from 5.0 to 150.0 $\mu\text{mol L}^{-1}$ and 100.0 to 800.0 $\mu\text{mol L}^{-1}$, respectively. LOD values of 0.70 $\mu\text{mol L}^{-1}$ (UA) and 31.6 $\mu\text{mol L}^{-1}$ (H_2O_2) were obtained. The GNP/PB structure was modified with GOx making the biosensor named GNP/PB/GOx, which was employed for the detection of glucose in synthetic sweat samples, with a LOD of 9.2 $\mu\text{mol L}^{-1}$. The biosensor provided great results, and its advantages, such as miniaturization, low-cost, and easy preparation make this biosensor very attractive in comparison to others presented in the literature. Furthermore, the biosensor showed an efficient performance, with the potential to be applied in biological samples, showing recoveries between $91.56\% \pm 3.91$ and $100.5\% \pm 0.46$ for the detection of glucose in artificial sweat. To show the versatility of the

proposed sensor, its performance as a wearable sensor was also evaluated towards the response of UA, as a proof-of-concept. The response obtained using the wearable wristband, in direct contact with the skin, showed a response similar to the obtained conventionally, with a decrease in the current peak of only 3%. Therefore, GNP/PB and GNP/PB/GOx are simple systems that present relevant characteristics, versatility, and efficient determination for UA, hydrogen peroxide, and glucose. In addition, the estimated cost per sensor unit was US\$ 0.91 and for the biosensor was US\$ 1.33, which makes these platforms attractive in the face of laboratory testing.

CRedit authorship contribution statement

Rodrigo Vieira Blasques: Investigation, Methodology, Data curation, Writing – original draft. **Jéssica S. Stefano:** Investigation, Conceptualization, Validation, Data curation, Writing – review & editing. **Jéssica R. Camargo:** Conceptualization, Validation, Data curation, Writing – review & editing. **Luiz R. Guterres e Silva:** Conceptualization, Validation, Writing – review & editing. **Laís Canniatti Brazaca:** Conceptualization, Validation, Data curation, Writing – review & editing. **Bruno Campos Janegitz:** Conceptualization, Visualization, Supervision, Project administration, Resources, Funding acquisition, Writing – review & editing.

Declaration of Competing Interest

The authors declare that they have no known competing financial interests or personal relationships that could have appeared to influence the work reported in this paper.

Acknowledgments

The authors are grateful to CNPq (303338/2019-9 and 120557/2019-3), CAPES (001 and 88887.636021/2021-00 and 88887.510880/2020-00), and FAPESP (2017/21097-3, 2018/19750-3 and 2019/23177-0) for the financial support.

Supplementary materials

Supplementary material associated with this article can be found, in the online version, at doi:10.1016/j.sn.2022.100118.

References

- [1] P.C. Ferreira, V.N. Ataíde, C.L. Silva Chagas, L. Angnes, W.K. Tomazelli Coltro, T. R. Longo Cesar Paixão, W.R. Araújo, Wearable electrochemical sensors for forensic and clinical applications, *TrAC Trends Anal. Chem.* 119 (2019), 115622.
- [2] J.S. Stefano, L.O. Orzari, H.A. Silva-Neto, V.N. de Ataíde, L.F. Mendes, W.K. T. Coltro, T.R. Longo Cesar Paixão, B.C. Janegitz, Different approaches for fabrication of low-cost electrochemical sensors, *Curr. Opin. Electrochem.* 32 (2022), 100893.
- [3] J.R. Camargo, L.O. Orzari, D.A.G. Araújo, P.R. de Oliveira, C. Kalinke, D.P. Rocha, A.L. Santos, R.M. Takeuchi, R.A. Abarza Muñoz, J.A. Bonacin, B.C. Janegitz, Development of conductive inks for electrochemical sensors and biosensors, *Microchem. J.* 164 (2021), 105998.
- [4] S.H. Ke, Q.W. Xue, C.Y. Pang, P.W. Guo, W.J. Yao, H.P. Zhu, W. Wu, Printing the ultra-long Ag nanowires inks onto the flexible textile substrate for stretchable electronics, *9*(2019) 686.
- [5] A.A. Arbab, A.A. Memon, K.C. Sun, J.Y. Choi, N. Mengal, I.A. Sahito, S.H. Jeong, Fabrication of conductive and printable nano carbon ink for wearable electronic and heating fabrics, *J. Colloid Interface Sci.* 539 (2019) 95–106.
- [6] L.O. Orzari, R. Cristina de Freitas, I. Aparecida de Araújo Andreotti, A. Gatti, B. C. Janegitz, A novel disposable self-adhesive inked paper device for electrochemical sensing of dopamine and serotonin neurotransmitters and biosensing of glucose, *Biosens. Bioelectron.* 138 (2019), 111310.
- [7] J.R. Camargo, T.A. Silva, G.A. Rivas, B.C. Janegitz, Novel eco-friendly water-based conductive ink for the preparation of disposable screen-printed electrodes for sensing and biosensing applications, *Electrochim. Acta* 409 (2022), 139968.
- [8] Y.Z.N. Htwe, M. Mariatti, Printed graphene and hybrid conductive inks for flexible, stretchable, and wearable electronics: progress, opportunities, and challenges, *J. Sci. Adv. Mater. Devices* 7 (2022), 100435.

- [9] P. Favaro, P. Bode, E.A. De Nadai Fernandes, Trace elements in nail polish as a source of contamination of nail clippings when used in epidemiological studies, *J. Radioanal. Nucl. Chem.* 264 (2005) 61–65.
- [10] T.N.H. Nguyen, J.K. Nolan, H. Park, S. Lam, M. Fattah, J.C. Page, H.E. Joe, M.B. G. Jun, H. Lee, S.J. Kim, R. Shi, H. Lee, Facile fabrication of flexible glutamate biosensor using direct writing of platinum nanoparticle-based nanocomposite ink, *Biosens. Bioelectron.* 131 (2019) 257–266.
- [11] H. Cankurtaran, E. Berber Karadayi, S. Sungur, Conductive composites of serigraphic inks and their usage in heavy metal sensor and biosensor, *Prog. Org. Coat.* 98 (2016) 6–9.
- [12] L.A. Pradela-Filho, D.A.G. Araújo, R.M. Takeuchi, A.L. Santos, Nail polish and carbon powder: an attractive mixture to prepare paper-based electrodes, *Electrochim. Acta* 258 (2017) 786–792.
- [13] I.A. de Araujo Andreotti, L.O. Orzari, J.R. Camargo, R.C. Faria, L.H. Marcolino-Junior, M.F. Bergamini, et al., Disposable and flexible electrochemical sensor made by recyclable material and low cost conductive ink, *J. Electroanal. Chem.* 840 (2019) 109–116.
- [14] M. Labib, E.H. Sargent, S.O. Kelley, Electrochemical methods for the analysis of clinically relevant biomolecules, *Chem. Rev.* 116 (2016) 9001–9090.
- [15] E.V. Karpova, E.V. Shcherbacheva, A.A. Galushin, D.V. Vokhmyanina, E. E. Karyakina, A.A. Karyakin, Noninvasive diabetes monitoring through continuous analysis of sweat using flow-through glucose biosensor, *Anal. Chem.* 91 (2019) 3778–3783.
- [16] J. Moyer, D. Wilson, I. Finkelshtein, B. Wong, R. Potts, Correlation between sweat glucose and blood glucose in subjects with diabetes, *Diabetes Technol. Ther.* 14 (2012) 398–402.
- [17] E.V. Karpova, E.V. Shcherbacheva, A.A. Galushin, D.V. Vokhmyanina, E. E. Karyakina, A.A. Karyakin, Noninvasive diabetes monitoring through continuous analysis of sweat using flow-through glucose biosensor, *Anal. Chem.* 91 (2019) 3778–3783.
- [18] J.X. Li, W.H. Zhang, Z.R. Tong, J.W. Liu, Fiber optic sensor modified by graphene oxide–glucose oxidase for glucose detection, *Opt. Commun.* 492 (2021), 126983.
- [19] A. Bener, A.O. Al-Hamaq, M. Öztürk, I. Tewfik, Vitamin D and elevated serum uric acid as novel predictors and prognostic markers for type 2 diabetes mellitus, *J. Pharm. Bioallied Sci.* 11 (2019) 127.
- [20] E. Krishnan, B.J. Pandya, L. Chung, A. Hariri, O. Dabbous, Hyperuricemia in young adults and risk of insulin resistance, prediabetes, and diabetes: a 15-year follow-up study, *Am. J. Epidemiol.* 176 (2012) 108–116.
- [21] A.F. Cicero, M. Rosticci, M. Bove, F. Fogacci, M. Giovannini, R. Urso, S. D'Addato, C. Borghi, Brisighella Heart Study Group, Serum uric acid change and modification of blood pressure and fasting plasma glucose in an overall healthy population sample: data from the Brisighella heart study, 49(2017) 275–82.
- [22] S. Husmann, E.S. Orth, A.J.G. Zarbin, A multi-technique approach towards the mechanistic investigation of the electrodeposition of Prussian blue over carbon nanotubes film, *Electrochim. Acta* 312 (2019) 380–391.
- [23] H. Susanto, A.M. Samsudin, N. Rokhati, I.N. Widiada, Immobilization of glucose oxidase on chitosan-based porous composite membranes and their potential use in biosensors, *Enzym. Microb. Technol.* 52 (2013) 386–392.
- [24] N.F.B. Azeredo, J.M. Gonçalves, P.O. Rossini, K. Araki, J. Wang, L. Angnes, Uric acid electrochemical sensing in biofluids based on Ni/Zn hydroxide nanocatalyst, *Microchim. Acta* 187 (2020) 379.
- [25] Y.X. Weng, Y.J. Jin, Q.Y. Meng, L. Wang, M. Zhang, Y.Z. Wang, Biodegradation behavior of poly(butylene adipate-co-terephthalate) (PBAT), poly(lactic acid) (PLA), and their blend under soil conditions, *Polym. Test.* 32 (2013) 918–926.
- [26] C.L.C. Carvalho, G. de Andrade Rodrigues, J.L. Magalhães, R.A. de Sousa Luz, E.T. S.G. da Silva, W. Cantanhede, Effect of Ibuprofen on the electrochemical properties of Prussian blue/single-walled carbon nanotubes nanocomposite modified electrode, *Surf. Interfaces* 25 (2021), 101276.
- [27] C. Amatore, N.Da Mota, C. Sella, L. Thouin, Theory and experiments of transport at channel microband electrodes under laminar flows. 1. Steady-state regimes at a single electrode, *Anal. Chem.* 79 (2007) 8502–8510.
- [28] Y. Li, M. Xu, P. Li, J. Dong, S. Ai, Nonenzymatic sensing of methyl parathion based on graphene/gadolinium Prussian Blue analogue nanocomposite modified glassy carbon electrode, *Anal. Methods* 6 (2014) 2157–2162.
- [29] A.J. Bard, L.R. Faulkner, *Student Solutions Manual to Accompany Electrochemical Methods: Fundamentals and Applications*, 2e, John Wiley & Sons, 2002.
- [30] Q. Yang, G. Rosati, V. Abarintos, M.A. Aroca, J.F. Osma, A. Merkoçi, Wearable and fully printed microfluidic nanosensor for sweat rate, conductivity, and copper detection with healthcare applications, *Biosens. Bioelectron.* 202 (2022), 114005.
- [31] S. Alankar, B.G. Vipin, Methods for the determination of limit of detection and limit of quantitation of the analytical methods, *Chron. Young Sci.* 2 (2011) 21–25.
- [32] F. Mazzara, B. Patella, G. Aiello, A. O'Riordan, C. Torino, A. Vilasi, R. Inguanta, Electrochemical detection of uric acid and ascorbic acid using r-GO/NPs based sensors, *Electrochim. Acta* 388 (2021), 138652.
- [33] H.D. Madhuchandra, B.E.K. Swamy, Electrochemical determination of Adrenaline and Uric acid at 2-Hydroxybenzimidazole modified carbon paste electrode Sensor: a voltammetric study, *Mater. Sci. Energy Technol.* 3 (2020) 464–471.
- [34] Q. Guan, H. Guo, R. Xue, M. Wang, X. Zhao, T. Fan, W. Yang, M. Xu, W. Yang, Electrochemical sensor based on covalent organic frameworks-MWCNT-NH₂/AuNPs for simultaneous detection of dopamine and uric acid, *J. Electroanal. Chem.* 880 (2021), 114932.
- [35] T.Q. Xu, Q.L. Zhang, J.N. Zheng, Z.Y. Lv, J. Wei, A.J. Wang, J.J. Feng, Simultaneous determination of dopamine and uric acid in the presence of ascorbic acid using Pt nanoparticles supported on reduced graphene oxide, *Electrochim. Acta* 115 (2014) 109–115.
- [36] L. Yang, D. Liu, J. Huang, T. You, Simultaneous determination of dopamine, ascorbic acid and uric acid at electrochemically reduced graphene oxide modified electrode, *Sens. Actuators B* 193 (2014) 166–172.
- [37] K. Cinková, K. Kianicková, D.M. Stanković, M. Vojs, M. Marton, L. Švorc, The doping level of boron-doped diamond electrodes affects the voltammetric sensing of uric acid, *Anal. Methods* 10 (2018) 991–996.
- [38] C.T. Huang, M.L. Chen, L.L. Huang, I.F. Mao, Uric acid and urea in human sweat, *Chin. J. Physiol.* 45 (2002) 109–115.
- [39] A.L. Hu, Y.H. Liu, H.H. Deng, G.L. Hong, A.L. Liu, X.H. Lin, X.H. Xia, W. Chean, Fluorescent hydrogen peroxide sensor based on cupric oxide nanoparticles and its application for glucose and L-lactate detection, *Biosens. Bioelectron.* 61 (2014) 374–378.
- [40] H. Yin, Y. Shi, Y. Dong, X. Chu, Synthesis of spinel-type CuGa₂O₄ nanoparticles as a sensitive non-enzymatic electrochemical sensor for hydrogen peroxide and glucose detection, *J. Electroanal. Chem.* 885 (2021), 115100.
- [41] O. Garate, L.S. Veiga, P. Tancredi, A.V. Medrano, L.N. Monsalve, G. Ybarra, High-performance non-enzymatic hydrogen peroxide electrochemical sensor prepared with a magnetite-loaded carbon nanotube waterborne ink, *J. Electroanal. Chem.* 915 (2022), 116372.
- [42] Y.F. Wei, X. Wang, W.J. Shi, R. Chen, L. Zheng, Z.Z. Wang, K. Chen, L. Gao, A novel methylenemalononitrile-BODIPY-based fluorescent probe for highly selective detection of hydrogen peroxide in living cells, *Eur. J. Med. Chem.* 226 (2021), 113828.
- [43] G.S. Cao, P. Wang, X.L.N. Li, Y.U.E. Wang, G. Wang, J. Li, A sensitive nonenzymatic hydrogen peroxide sensor based on Fe₃O₄-Fe₂O₃ nanocomposites, *Bull. Mater. Sci.* 38 (2015) 163–167.
- [44] M. Şenel, E. Çevik, M.F. Abasiyanik, Amperometric hydrogen peroxide biosensor based on covalent immobilization of horseradish peroxidase on ferrocene containing polymeric mediator, *Sens. Actuators B* 145 (2010) 444–450.
- [45] K.K. Lee, P.Y. Loh, C.H. Sow, W.S. Chin, CoOOH nanosheet electrodes: simple fabrication for sensitive electrochemical sensing of hydrogen peroxide and hydrazine, *Biosens. Bioelectron.* 39 (2013) 255–260.
- [46] Y. Wang, X. Ma, Y. Wen, Y. Xing, Z. Zhang, H. Yang, Direct electrochemistry and bioelectrocatalysis of horseradish peroxidase based on gold nano-seeds dotted TiO₂ nanocomposite, *Biosens. Bioelectron.* 25 (2010) 2442–2446.
- [47] K. Atacan, M. Özacar, Construction of a non-enzymatic electrochemical sensor based on CuO/g-C₃N₄ composite for selective detection of hydrogen peroxide, *Mater. Chem. Phys.* 266 (2021), 124527.
- [48] D.M. Liu, J. Chen, Y.P. Shi, Advances on methods and easy separated support materials for enzymes immobilization, *TrAC Trends Anal. Chem.* 102 (2018) 332–342.
- [49] X. Jin, F. Xi, D. Lv, Q. Wu, X. Lin, The effect of the chitosan membrane properties on the enzyme adsorption and performance for the construction of horseradish peroxidase biosensors, *Carbohydr. Polym.* 85 (2011) 786–791.
- [50] B. Wu, G. Zhang, S. Shuang, M.M.F. Choi, Biosensors for determination of glucose with glucose oxidase immobilized on an eggshell membrane, *Talanta* 64 (2004) 546–553.
- [51] S. Banerjee, P. Sarkar, A.P.F. Turner, Amperometric biosensor based on Prussian Blue nanoparticle-modified screen-printed electrode for estimation of glucose-6-phosphate, *Anal. Biochem.* 439 (2013) 194–200.
- [52] N. Chandra Sekar, S.A. Mousavi Shaeigh, S.H. Ng, L. Ge, S.N. Tan, A paper-based amperometric glucose biosensor developed with Prussian Blue-modified screen-printed electrodes, *Sens. Actuators B* 204 (2014) 414–420.
- [53] Y. Zhang, Y. Liu, Z. Chu, L. Shi, W. Jin, Amperometric glucose biosensor based on direct assembly of Prussian blue film with ionic liquid-chitosan matrix assisted enzyme immobilization, *Sens. Actuators B* 176 (2013) 978–984.
- [54] D. Jiang, Z. Chu, J. Peng, W. Jin, Screen-printed biosensor chips with Prussian blue nanocubes for the detection of physiological analytes, *Sens. Actuators B* 228 (2016) 679–687.
- [55] E.M.I.M. Ekanayake, D.M.G. Preethichandra, K. Kaneto, Polypyrrole nanotube array sensor for enhanced adsorption of glucose oxidase in glucose biosensors, *Biosens. Bioelectron.* 23 (2007) 107–113.
- [56] K. Vijayaraj, S.W. Hong, S.H. Jin, S.C. Chang, D.S. Park, Fabrication of a novel disposable glucose biosensor using an electrochemically reduced graphene oxide–glucose oxidase biocomposite, *J. Anal. Methods* 8 (2016) 6974–6981.
- [57] A. Jedrzak, M. Kuznowicz, T. Rebiś, T. Jesionowski, Portable glucose biosensor based on polynorepinephrine@magnetite nanomaterial integrated with a smartphone analyzer for point-of-care application, *Bioelectrochemistry* 145 (2022), 108071.
- [58] M. Şenel, Simple method for preparing glucose biosensor based on *in-situ* polypyrrole cross-linked chitosan/glucose oxidase/gold bionanocomposite film, *Mater. Sci. Eng. C* 48 (2015) 287–293.
- [59] A. Jedrzak, T. Rebiś, L. Klapiszewski, J. Zdarta, G. Milczarek, T. Jesionowski, Carbon paste electrode based on functional GOx/silica-lignin system to prepare an amperometric glucose biosensor, *Sens. Actuators B* 256 (2018) 176–185.
- [60] E. Witkowska Nery, M. Kundys, P.S. Jelen, M. Jönsson-Niedziółka, Electrochemical glucose sensing: is there still room for improvement? *Anal. Chem.* 88 (2016) 11271–11282.
- [61] Z. Tang, X. Du, R.F. Louie, G.J. Kost, Effects of drugs on glucose measurements with handheld glucose meters and a portable glucose analyzer, *Am. J. Clin. Pathol.* 113 (2000) 75–86.
- [62] C.J. Yuan, C.L. Hsu, S.C. Wang, K.S. Chang, Eliminating the interference of ascorbic acid and uric acid to the amperometric glucose biosensor by cation exchangers membrane and size exclusion membrane, *Electroanalysis* 17 (2005) 2239–2245.
- [63] J. Wang, J. Liu, L. Chen, F. Lu, Highly selective membrane-free, mediator-free glucose biosensor, *Anal. Chem.* 66 (1994) 3600–3603.

- [64] J.D. Newman, S.F. White, I.E. Tothill, A.P.F. Turner, Catalytic materials, membranes, and fabrication technologies suitable for the construction of amperometric biosensors, *Anal. Chem.* 67 (1995) 4594–4599.
- [65] M.A.T. Gilmartin, J.P. Hart, D.T. Patton, Prototype, solid-phase, glucose biosensor, *Analyst* 120 (1995) 1973–1981.
- [66] J. Wang, T. Golden, Metalloporphyrin chemically modified glassy carbon electrodes as catalytic voltammetric sensors, *Anal. Chim. Acta* 217 (1989) 343–351.
- [67] C.F. Hogan, R.J. Forster, Mediated electron transfer for electroanalysis: transport and kinetics in tin films of [Ru (bpy)₂PVP10] (ClO₄)₂, *Anal. Chim. Acta* 396 (1999) 13–21.
- [68] W.Z. Jia, K. Wang, X.H. Xia, Elimination of electrochemical interferences in glucose biosensors, *TrAC Trends Anal. Chem.* 29 (2010) 306–318.
- [69] L.C. Brazaca, C.B. Bramorski, J. Cancino-Bernardi, S. da Silveira Cruz-Machado, R. P. Markus, B.C. Janegitz, V. Zucolotto, An antibody-based platform for melatonin quantification, *Colloids Surf. B* 171 (2018) 94–100.
- [70] B.C. Kang, B.S. Park, T.J. Ha, Highly sensitive wearable glucose sensor systems based on functionalized single-wall carbon nanotubes with glucose oxidase-nafion composites, *Appl. Surf. Sci.* 470 (2019) 13–18.
- [71] W. He, C. Wang, H. Wang, M. Jian, W. Lu, X. Liang, X. Zhang, F. Yang, Y., Zhang, Integrated textile sensor patch for real-time and multiplex sweat analysis, 5(2019) eaax0649.
- [72] J. Kim, A.S. Campbell, B.E.F. de Ávila, J. Wang, Wearable biosensors for healthcare monitoring, *Nat. Biotechnol.* 37 (2019) 389–406.
- [73] J.S. Stefano, C. Kalinke, R.G. da Rocha, D.P. Rocha, V.A.O.P. da Silva, J.A. Bonacin, L. Angnes, E.M. Richter, B.C. Janegitz, R.A. Abarza Muñoz, Electrochemical (Bio) sensors enabled by fused deposition modeling-based 3D printing: a guide to selecting designs, printing parameters, and post-treatment protocols, *Anal. Chem.* 94 (2022) 6417–6429.
- [74] R.M. Cardoso, C. Kalinke, R.G. Rocha, P.L. dos Santos, D.P. Rocha, P.R. Oliveira, B. C. Janegitz, J.A. Bonacin, E.M. Richter, R.A. Abarza Muñoz, Additive-manufactured (3D-printed) electrochemical sensors: a critical review, *Anal. Chim. Acta* 1118 (2020) 73–91.
- [75] A. Kalkal, S. Kumar, P. Kumar, R. Pradhan, M. Willander, G. Packirisamy, S. Kumar, B.D. Malhotra, Recent advances in 3D printing technologies for wearable (bio)sensors, *Addit. Manuf.* 46 (2021), 102088.
- [76] Y. Yang, Y. Song, X. Bo, J. Min, O.S. Pak, L. Zhu, L. Zhu, M. Wang, J. Tu, A. Kogan, H. Zhang, T.K. Hsiai, Z. Li, W. Gao, A laser-engraved wearable sensor for sensitive detection of uric acid and tyrosine in sweat, *Nat. Biotechnol.* 38 (2020) 217–224.
- [77] J.S. Stefano, E.S.L.R. Guterres, R.G. Rocha, L.C. Brazaca, E.M. Richter, R.A. Abarza Muñoz, B.C. Janegitz, New conductive filament ready-to-use for 3D-printing electrochemical (bio)sensors: towards the detection of SARS-CoV-2, *Anal. Chim. Acta* 1191 (2022), 339372.
- [78] B.M.R. Appenzeller, C. Schummer, S.B. Rodrigues, R. Wennig, Determination of the volume of sweat accumulated in a sweat-patch using sodium and potassium as internal reference, *J. Chromatogr. B* 852 (2007) 333–337.
- [79] F.W. Booth, C.K. Roberts, M.J. Laye, Lack of exercise is a major cause of chronic diseases, *Compr. Physiol.* 2 (2012) 1143–1211.